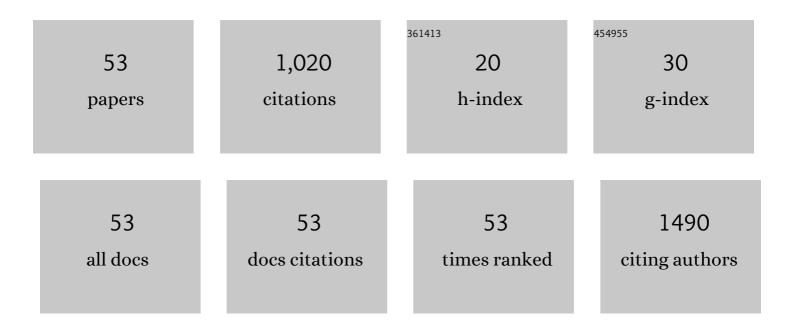
Yiming Bai

List of Publications by Year in descending order

Source: https://exaly.com/author-pdf/9392341/publications.pdf Version: 2024-02-01



VIMING RAL

#	Article	IF	CITATIONS
1	Recent Advances of Monolithic <scp>Allâ€Perovskite</scp> Tandem Solar Cells: From Materials to Devices. Chinese Journal of Chemistry, 2022, 40, 856-871.	4.9	11
2	Balance PCE, AVT and CRI for good eye comfort semi-transparent organic photovoltaics via Ga2O3 or In2O3 electron collection layers. Organic Electronics, 2022, , 106572.	2.6	2
3	Ternary blend strategy in benzotriazole-based organic photovoltaics for indoor application. Green Energy and Environment, 2021, 6, 920-928.	8.7	23
4	Efficient organic solar cells with low-temperature in situ prepared Ga2O3 or In2O3 electron collection layers. Science China Materials, 2021, 64, 1095-1104.	6.3	5
5	Highly Efficient and Super Stable Fullâ€Color Quantum Dots Lightâ€Emitting Diodes with Solutionâ€Processed Allâ€Inorganic Charge Transport Layers. Small, 2021, 17, e2007363.	10.0	32
6	Quantifying charge transportation for stable organic solar cells with a novel aluminum acetylacetone electron collection layer. Organic Electronics, 2021, 95, 106182.	2.6	2
7	Size-Controllable Metal Chelates as Both Light Scattering Centers and Electron Collection Layer for High-Performance Polymer Solar Cells. CCS Chemistry, 2021, 3, 37-49.	7.8	12
8	Strategies Toward Extending the Nearâ€Infrared Photovoltaic Response of Perovskite Solar Cells. Solar Rrl, 2020, 4, 1900280.	5.8	13
9	Water-Soluble SnO ₂ Nanoparticles as the Electron Collection Layer for Efficient and Stable Inverted Organic Tandem Solar Cells. ACS Applied Energy Materials, 2020, 3, 12662-12671.	5.1	12
10	High Performance Tandem Solar Cells with Inorganic Perovskite and Organic Conjugated Molecules to Realize Complementary Absorption. Journal of Physical Chemistry Letters, 2020, 11, 9596-9604.	4.6	35
11	Printable SnO2 cathode interlayer with up to 500 nm thickness-tolerance for high-performance and large-area organic solar cells. Science China Chemistry, 2020, 63, 957-965.	8.2	38
12	Novel cathode buffer layer of Al(acac) ₃ enables efficient, large area and stable semi-transparent organic solar cells. Materials Chemistry Frontiers, 2020, 4, 2072-2080.	5.9	22
13	Facile Method of Solvent-Flushing To Building Component Distribution within Photoactive Layers for High-Performance Organic Solar Cells. ACS Applied Materials & Interfaces, 2020, 12, 31459-31466.	8.0	10
14	High Performance Quasiâ€2D Perovskite Skyâ€Blue Lightâ€Emitting Diodes Using a Dualâ€Ligand Strategy. Small, 2020, 16, e2002940.	10.0	65
15	Low-temperature in-situ preparation of ZnO electron extraction layer for efficient inverted polymer solar cells. Organic Electronics, 2019, 74, 82-88.	2.6	18
16	Expanding the Light Harvesting of CsPbl ₂ Br to Near Infrared by Integrating with Organic Bulk Heterojunction for Efficient and Stable Solar Cells. ACS Applied Materials & Interfaces, 2019, 11, 37991-37998.	8.0	25
17	Enhancing charge transport in an organic photoactive layer <i>via</i> vertical component engineering for efficient perovskite/organic integrated solar cells. Nanoscale, 2019, 11, 4035-4043.	5.6	22
18	Multifunctional bipyramid-Au@ZnO core–shell nanoparticles as a cathode buffer layer for efficient non-fullerene inverted polymer solar cells with improved near-infrared photoresponse. Journal of Materials Chemistry A, 2019, 7, 2667-2676.	10.3	27

Yiming Bai

#	Article	lF	CITATIONS
19	Interfacial engineering and optical coupling for multicolored semitransparent inverted organic photovoltaics with a record efficiency of over 12%. Journal of Materials Chemistry A, 2019, 7, 15887-15894.	10.3	83
20	Tandem structure: a breakthrough in power conversion efficiency for highly efficient polymer solar cells. Sustainable Energy and Fuels, 2019, 3, 910-934.	4.9	28
21	Enhancing the electron blocking ability of n-type MoO3 by doping with p-type NiO for efficient nonfullerene polymer solar cells. Organic Electronics, 2019, 68, 168-175.	2.6	31
22	Semitransparent solar cells with over 12% efficiency based on a new low bandgap fluorinated small molecule acceptor. Materials Chemistry Frontiers, 2019, 3, 2483-2490.	5.9	55
23	Boosting photocurrent of GaInP top-cell for current-matched III–V monolithic multiple-junction solar cells via plasmonic decahedral-shaped Au nanoparticles. Solar Energy, 2018, 166, 181-186.	6.1	8
24	Extending absorption of near-infrared wavelength range for high efficiency CIGS solar cell via adjusting energy band. Current Applied Physics, 2018, 18, 484-490.	2.4	31
25	Synergy of a titanium chelate electron collection layer and a vertical phase separated photoactive layer for efficient inverted polymer solar cells. Journal of Materials Chemistry A, 2018, 6, 7257-7264.	10.3	20
26	Broadening the Photoresponse to Nearâ€Infrared Region by Cooperating Fullerene and Nonfullerene Acceptors for High Performance Ternary Polymer Solar Cells. Macromolecular Rapid Communications, 2018, 39, 1700492.	3.9	10
27	Solutionâ€Processed Titanium Chelate Used as Both Electrode Modification Layer and Intermediate Layer for Efficient Inverted Tandem Polymer Solar Cells. Chinese Journal of Chemistry, 2018, 36, 194-198.	4.9	19
28	Bright prospect of using alcohol-soluble Nb2O5 as anode buffer layer for efficient polymer solar cells based on fullerene and non-fullerene acceptors. Organic Electronics, 2018, 52, 323-328.	2.6	14
29	Efficient Polymer Solar Cells with Alcohol-Soluble Zirconium(IV) Isopropoxide Cathode Buffer Layer. Energies, 2018, 11, 328.	3.1	6
30	Preparation and mechanismÂanalysis ofÂpolycrystalline silicon thin films withÂpreferred orientation on graphite substrate. Journal of Materials Science: Materials in Electronics, 2018, 29, 1377-1383.	2.2	4
31	Constructing Desired Vertical Component Distribution Within a PBDB-T:ITIC-M Photoactive Layer via Fine-Tuning the Surface Free Energy of a Titanium Chelate Cathode Buffer Layer. Frontiers in Chemistry, 2018, 6, 292.	3.6	21
32	Perfect Complementary in Absorption Spectra with Fullerene, Nonfullerene Acceptors and Medium Band Gap Donor for High-Performance Ternary Polymer Solar Cells. ACS Applied Materials & Interfaces, 2018, 10, 29831-29839.	8.0	15
33	Fine Tuning the Light Distribution within the Photoactive Layer by Both Solutionâ€Processed Anode and Cathode Interlayers for High Performance Polymer Solar Cells. Solar Rrl, 2018, 2, 1800141.	5.8	10
34	Enhanced Electron Injection and Exciton Confinement for Pure Blue Quantum-Dot Light-Emitting Diodes by Introducing Partially Oxidized Aluminum Cathode. Journal of Visualized Experiments, 2018, , .	0.3	1
35	Decahedral-shaped Au nanoparticles as plasmonic centers for high performance polymer solar cells. Organic Electronics, 2017, 43, 33-40.	2.6	24
36	Effect of Energy Alignment, Electron Mobility, and Film Morphology of Perylene Diimide Based Polymers as Electron Transport Layer on the Performance of Perovskite Solar Cells. ACS Applied Materials & Interfaces, 2017, 9, 10983-10991.	8.0	76

Yiming Bai

#	Article	IF	CITATIONS
37	Pure Blue and Highly Luminescent Quantumâ€Dot Lightâ€Emitting Diodes with Enhanced Electron Injection and Exciton Confinement via Partially Oxidized Aluminum Cathode. Advanced Optical Materials, 2017, 5, 1700035.	7.3	39
38	Incorporating an Electrode Modification Layer with a Vertical Phase Separated Photoactive Layer for Efficient and Stable Inverted Nonfullerene Polymer Solar Cells. ACS Applied Materials & Interfaces, 2017, 9, 43871-43879.	8.0	23
39	Efficient Planar Structured Perovskite Solar Cells with Enhanced Open-Circuit Voltage and Suppressed Charge Recombination Based on a Slow Grown Perovskite Layer from Lead Acetate Precursor. ACS Applied Materials & Interfaces, 2017, 9, 41937-41944.	8.0	23
40	The Effect of Donor and Nonfullerene Acceptor Inhomogeneous Distribution within the Photoactive Layer on the Performance of Polymer Solar Cells with Different Device Structures. Polymers, 2017, 9, 571.	4.5	18
41	Blue LEDs: Pure Blue and Highly Luminescent Quantumâ€Dot Lightâ€Emitting Diodes with Enhanced Electron Injection and Exciton Confinement via Partially Oxidized Aluminum Cathode (Advanced) Tj ETQq1 1 0.78	4 3.3 4 rgB1	ſ ¦ Øverlock
42	Enhancing the Photocurrent of Top-Cell by Ellipsoidal Silver Nanoparticles: Towards Current-Matched GaInP/GaInAs/Ge Triple-Junction Solar Cells. Nanomaterials, 2016, 6, 98.	4.1	6
43	Performance Analysis of a Grid-connected High Concentrating Photovoltaic System under Practical Operation Conditions. Energies, 2016, 9, 117.	3.1	9
44	Regular Hexagonal Gold Nanoprisms Fabricated by a Physical Method: Toward Use as Ultrasensitive Surfaceâ€Enhanced Raman Scattering Substrates. Particle and Particle Systems Characterization, 2016, 33, 254-260.	2.3	5
45	Diversity in plasma arrival sequence correlated to oxygen deficiencies of oxide thin films grown by PLD. Science China Materials, 2015, 58, 269-273.	6.3	0
46	Elimination of small-sized Ag nanoparticles via rapid thermal annealing for high efficiency light trapping structure. Applied Surface Science, 2014, 315, 1-7.	6.1	20
47	Ag nanoparticles preparation and their light trapping performance. Science China Technological Sciences, 2013, 56, 109-114.	4.0	8
48	Sol-Gel Preparation, Characterization, and Photocatalytic Activity of Macroporous TiO2 Thin Films. Journal of the American Ceramic Society, 2011, 94, 1191-1197.	3.8	13
49	Improved performance of GaAs-based micro-solar cell with novel polyimide/SiO2/TiAu/SiO2 structure. Science China Technological Sciences, 2011, 54, 830-834.	4.0	1
50	Quantifying the effectiveness of SiO2/Au light trapping nanoshells for thin film poly-Si solar cells. Science China Technological Sciences, 2010, 53, 2228-2231.	4.0	3
51	Evaluating the effect of dislocation on the photovoltaic performance of metamorphic tandem solar cells. Science China Technological Sciences, 2010, 53, 2569-2574.	4.0	8
52	Aluminum induced crystallization of strongly (111) oriented polycrystalline silicon thin film and nucleation analysis. Science China Technological Sciences, 2010, 53, 3002-3005.	4.0	5
53	Highâ€Efficiency Microcavity Semitransparent Organic Photovoltaics with Simultaneously Improved Average Visible Transmittance and Color Rendering Index. Solar Rrl, 0, , 2200174.	5.8	8